

## Three-dimensional phase boundary estimation in sedimentation process using electrical impedance tomography with the aid of unscented Kalman filter

Anil Kumar Khambampati<sup>1</sup>, Ahmar Rashid<sup>1</sup>, Jeong Seong Lee<sup>2</sup>, Sin Kim<sup>2</sup> and Kyung Youn Kim<sup>1\*</sup>

<sup>1</sup>Department of Electronic Engineering, Cheju National University,  
Cheju 690-756, South Korea

<sup>2</sup>Department of Nuclear and Energy Engineering, Cheju National University  
Cheju 690-756, South Korea

E-mail: <sup>1</sup>anil@cheju.ac.kr, ahmar.rashid@gmail.com, kyungyk@cheju.ac.kr, <sup>2</sup>jslee@cheju.ac.kr, sinkim@cheju.ac.kr.

**Abstract:** This work is related to interfacial phase boundary estimation in sedimentation monitoring using electrical impedance tomography. The fluid is assumed to settle into three different phases separated by sharp interfacial boundary. The time evolution of the phase interface gives important information about the sedimentation process which can be used to control and optimize the sedimentation process. Phase interface location and their corresponding conductivities estimation is treated as a stochastic nonlinear state estimation problem with the nonstationary interfacial phase boundary (state) being estimated online with the aid of unscented Kalman filter. Numerical experiments are performed to evaluate the performance of the proposed approach and is compared with conventional extended Kalman filter.

### 1. Introduction

Settling of the suspensions in settling tanks has attracted much attention. In sedimentation process solid-fluid suspension is separated into its components under the influence of gravity. It is widely used in many industrial processes such as mining, waste water treatment and pulp and paper industry [4,5]. Sedimentation monitoring provides information about the properties of sediments and thus can be used to control and optimize the industrial processes. In the modeling of sedimentation process, fluid is assumed to settle into three different layers. The top layer is clear liquid, the middle is dilute slurry where the actual sedimentation takes place by unhindered settling and the bottom layer is a compact layer where hindered settling occurs. These layers settle with a velocity which is assumed to be a function of the solid composition of the layers. The phase interface location with respect to time is termed as the settling curves and the rate of change of these settling curves gives rise to settling velocities. These parameters provide necessary information about the sedimentation process [2,3]. Several measurement techniques have been employed to obtain settling curves and velocities. These include light based techniques, image processing tools and electrical methods. Electrical methods do not require any additional models to obtain parameters such as conductivity. Also, another major advantage with the electrical methods is that transparent sedimentation tanks are not needed unlike the other measurement techniques. Considering the advantages of the electrical methods over other techniques, electrical impedance tomography (EIT) has been used in sedimentation monitoring [6,7]. In EIT, a set of electric currents are passed through the electrodes mounted on the

surface of the object to be imaged and the excited voltages are measured. Based on the current-voltage relationship, internal conductivity distribution is reconstructed.

Reconstruction algorithms for EIT can be classified into static and dynamic imaging techniques. The former technique, usually employed for time invariant internal conductivity distribution, often fails when there are fast impedance changes. The later technique enhances the temporal resolution for situations where the conductivity distribution inside the body changes rapidly. One of the most widely used dynamic algorithms for nonlinear systems is Extended Kalman filter (EKF). However, it requires calculating the Jacobian matrix which is not always available. It is difficult to implement, difficult to tune, and is only reliable for systems that are almost linear on the time scale of the updates.

In this paper we introduce an effective way to estimate the sharp interfacial phase boundaries in three-dimensional sedimentation monitoring using electrical impedance tomography with the aid of unscented Kalman filter (UKF). Unscented Kalman filter uses unscented transform to propagate mean and covariance information through a nonlinear transformation [1]. To locate the interfacial phase boundaries we use first-order kinematic model as an evolution model for better estimation of settling velocities. Kinematic models popularly used in motion tracking can be used as an appropriate evolution model for parameters changing with constant velocity between the measurements [2,8,9].

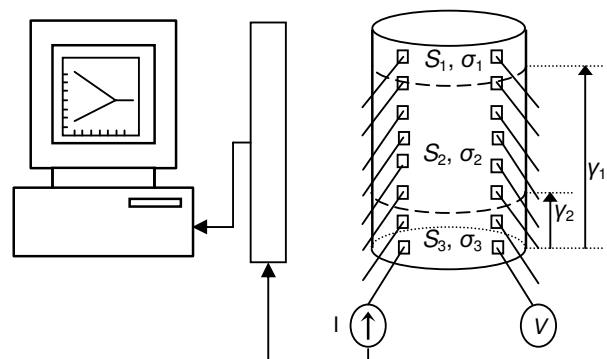


Figure 1. Schematic layout for sedimentation monitoring using EIT. The measurement electrodes are denoted by the square patch on the surface of the phantom.  $S_k$  denotes the  $k$ th sub region with different phases,  $\sigma_k$  denotes the conductivity of the  $k$ th phase,  $y_k$  denotes location of  $k$ th interface.

## 2. Mathematical model

In sedimentation monitoring using EIT, electrical currents are injected into the electrodes attached on the periphery of the sedimentation tank. When electrical currents are  $I_l (l=1,2,\dots,L)$  injected into the object  $\Omega \in \mathfrak{R}^3$  through the electrodes  $e_l (l=1,2,\dots,L)$  attached on the boundary  $\partial\Omega$  with the internal structure, the conductivity distribution  $\sigma$  is known for  $\Omega$ , then corresponding electrical potential  $u$  on the  $\Omega$  can be determined uniquely from the partial differential equation, which can be derived from the Maxwell equations as

$$\nabla \cdot (\sigma \nabla u) = 0 \text{ in } \Omega \quad (1)$$

with the following boundary conditions based on the complete electrode model:

$$u + z_l \sigma \frac{\partial u}{\partial n} = \bar{U}_l \text{ on } e_l, l=1,2,\dots,L \quad (2)$$

$$\int_{e_l} \sigma \frac{\partial u}{\partial n} dS = \bar{I}_l, l=1,2,\dots,L \quad (3)$$

$$\sigma \frac{\partial u}{\partial n} = 0 \text{ on } \partial\Omega \setminus \bigcup_{l=1}^L e_l \quad (4)$$

where  $z_l$  is the effective contact impedance between  $l$ th electrode and electrolyte,  $\bar{U}_l = \bar{U}_l(t_k)$  is the potential on the  $l$ th electrode at time  $k$ ,  $\bar{I}_l = \bar{I}_l(t_k)$  is the injected current on the  $l$ th electrode at time  $k$ ,  $e_l$  is  $l$ th electrode,  $n$  is outward unit normal, and  $L$  is the total number of electrodes. Furthermore, the following two constraints for the injected currents and measured voltages are needed to ensure the existence and uniqueness of the solution:

one is using the conservation of charge

$$\sum_{l=1}^L \bar{I}_l = 0 \quad (5)$$

and by choosing the ground electrode such that

$$\sum_{l=1}^L \bar{U}_l = 0 \quad (6)$$

The computation of the potential  $u$  on  $\Omega$  and voltages  $\bar{U}_l$  on the electrodes for the given conductivity distribution  $\sigma$  and boundary conditions is called the forward problem. In general, the forward problem cannot be solved analytically, thus we have to resort to the numerical method. In this paper, we used the FEM to obtain numerical solution. For more details on the forward solution and the FEM approach, see [2].

## 3. Boundary representation

In this section we describe the shape parameterization of the phase interface for the sedimentation model shown in Figure 1. Sedimentation tank consists of three layers of different phases separated by sharp interfaces. The conductivity function are parameterized by the location of the phases interfaces ( $\gamma_k, k=1,2$ ) and the conductivities of the phase layers ( $\sigma_k, k=1,2,3$ ). The phase interface  $C_q$  at location  $\gamma_q$  can be represented by a horizontal plane as

$$C_q(\gamma_q) = \{w \in \mathfrak{R}^3 (w - r_q)^T n = 0\}, \quad (7)$$

where  $n = (0,0,1)^T$  is the normal vector of the plane and the position vector is of the form  $r_q = (0,0,\gamma_q)^T$ . Here, apart from the conductivities, the phase interface is also ioestimated. Therefore, the forward solver has to be modified. Let us assume that the region  $\Omega$  is divided into disjoint regions  $S_k$  given by,

$$\Omega = \bigcup_{k=1}^3 S_k \quad (8)$$

where three regions exist in domain as shown in Figure 1. If  $\chi_k(r)$  denotes the characteristic function of subregion  $S_k$ , we can express the conductivities of each layer as

$$\sigma = \sum_{k=0}^p \sigma_k \chi_k(r) \quad (9)$$

This parameterization effects the system matrix in FEM formulation. The complete description of this FEM formulation in this regard can be found in [2,3].

## 4. Inverse problem

The inverse problem here is to estimate the time-varying interface location, velocities of the interface along with the conductivity distribution inside the object based on the injected currents and the measured voltages. We consider the underlying inverse problem as a state estimation problem to estimate rapidly time-varying distribution inside the domain. In the state estimation problem, we need the so-called dynamic model which consists of the state equation, i.e., the temporal evolution of the state and the observation equation, i.e., the relationship between the state and boundary voltage.

First of all, consider the state evolution model. Here, the state equation is assumed to be of multiple linear form with different process noise [2].

$$x_{k+1} = F_k x_k + D_k w_k \quad (11)$$

where  $F_k \in \mathfrak{R}^{N \times N}$  is the state transition matrix,  $N$  is the number of unknown state parameters,  $w$  is the process noise (assumed zero mean Gaussian noise) and  $D_k$  represent the transition matrix of the process noise. The measurement equation corresponding to boundary voltages is given by

$$\bar{U}_k = h_k(x_k) + v_k \quad (12)$$

where  $h_k(x_k)$  represents the forward solution through FEM and  $v$  represents the measurement noise governed by zero mean Gaussian noise.

### 4.1 Formulation of extended Kalman filter

In Kalman filtering we estimate the state  $x_k$  based on all the measurements taken up to the time  $kT$ . With the Gaussian assumptions, the required estimate is obtained by minimizing the cost functional which is formulated based on the above state and measurements equations (11) and (12) respectively. The cost functional for the extended Kalman filter EKF is of the form

$$G(x_k) = \frac{1}{2} [\|x_k - x_{k|k-1}\| (\tau_{k|k-1})^{-1}] \quad (13)$$

where  $\|x\|_R$  denotes  $x^T R x$ ,  $\tau_{k|k-1} \equiv E[(x_k - x_{k|k-1})(x_k - x_{k|k-1})^T]$

Minimizing the cost functional (13) and solving for the updates of the associated covariance matrices, we obtain the recursive extended Kalman filter algorithm for each model, which consists of the following steps

$$x_{k|k-1} = F_{k-1} x_{k-1|k-1} \quad (14)$$

$$\Gamma_{k|k-1} = F_{k-1} x_{k-1|k-1} (F_{k-1})^T + D_{k-1} Q_{k-1} D_{k-1}^T \quad (15)$$

$$K_k = \Gamma_{k|k-1} (J_k)^T (J_k \Gamma_{k|k-1} J_k^T + R_k)^{-1} \quad (16)$$

$$x_{k|k} = x_{k|k-1} + K_k (\bar{U} - h_k(x_{k|k-1})) \quad (17)$$

$$\Gamma_{k|k} = (I_N - K_k J_k) \Gamma_{k|k-1} \quad (18)$$

where  $J_k$  represents the Jacobian with respect to the previous state. One of the main task in Inverse solver is the computation of Jacobian. The detailed description of obtaining Jacobian can be seen in [2,3].

#### 4. 2 Formulation of unscented Kalman filter

In contrast to the EKF, which makes use of a Gaussian random variable (GRV) to estimate the state distribution and linearizes it using Jacobian matrices, which is prone to large errors, the unscented Kalman filter (UKF) uses a deterministic sample-and-propagate approach to capture the mean and variance estimates. The underlying algorithm for the UKF is explained as follows[1]:

Initialize with:

$$\begin{aligned} \hat{x}_0 &= E[x_0] \\ P_0 &= E[(x_0 - \hat{x}_0)(x_0 - \hat{x}_0)^T] \end{aligned} \quad (19)$$

For  $k \in \{1, \dots, \infty\}$ , calculate the sigma points:

$$x_{k-1} = \left[ \hat{x}_{k-1} \quad \hat{x}_{k-1} + \gamma \sqrt{P_{k-1}} \quad \hat{x}_{k-1} - \gamma \sqrt{P_{k-1}} \right] \quad (20)$$

Time Update:

$$x_{k|k-1} = F[x_{k-1}, u_{k-1}] \quad (21)$$

$$\hat{x}_k^- = \sum_{i=0}^{2M} W_i^{(m)} x_{i,k|k-1} \quad (22)$$

$$P_k^- = \sum_{i=0}^{2M} W_i^{(c)} [x_{i,k|k-1} - \hat{x}_k^-][x_{i,k|k-1} - \hat{x}_k^-]^T + Q_k \quad (23)$$

$$y_{k|k-1} = H[x_{k|k-1}] \quad (24)$$

$$\hat{y}_k^- = \sum_{i=0}^{2M} W_i^{(m)} y_{i,k|k-1} \quad (25)$$

Measurement Update:

$$P_{\hat{y}_k \hat{y}_k} = \sum_{i=0}^{2M} W_i^{(c)} [y_{i,k|k-1} - \hat{y}_k^-][y_{i,k|k-1} - \hat{y}_k^-]^T + R_k \quad (26)$$

$$P_{x_k y_k} = \sum_{i=0}^{2M} W_i^{(c)} [x_{i,k|k-1} - \hat{x}_k^-][y_{i,k|k-1} - \hat{y}_k^-]^T \quad (27)$$

$$K_k = P_{x_k y_k} P_{\hat{y}_k \hat{y}_k}^{-1} \quad (28)$$

$$\hat{x}_k = \hat{x}_k^- + K_k (y_k - \hat{y}_k^-) \quad (29)$$

$$P_k = P_k^- - K_k P_{\hat{y}_k \hat{y}_k} K_k^T \quad (30)$$

where  $M$  is dimension of the state vector,  $\gamma = \sqrt{(M + \lambda)}$ ,  $\lambda = \alpha^2(M + k) - M$  is the composite scaling parameter and  $\alpha$  is another scaling parameter which determines the spread of the sigma points.  $Q_k$  is the process noise covariance and  $R_k$  is the measurement noise covariance.  $W_i$  are the weights defined as follows:

$$W_0^{(m)} = \frac{\lambda}{(M + \lambda)} \quad (31)$$

$$W_0^{(c)} = \frac{\lambda}{(M + \lambda)} + (1 - \alpha^2 + \beta) \quad (32)$$

$$W_i^{(c)} = W_i^{(m)} = \frac{1}{2(M + \lambda)}, i = 1 \dots 2M \quad (33)$$

Here,  $\beta$  is used to incorporate a prior knowledge of the distribution of  $x$ .

### 5. Results and discussion

Numerical experiments were carried out with the sedimentation model shown in Figure 1. The tank is composed of 32 electrodes arranged in four vertical arrays of eight electrodes each. The size of the electrode is 1 cm x 1 cm and the vertical separation between the electrodes center is 2.5 cm. A simple current injection protocol composed of four current injections is used. In each current injection, current is injected through top and bottom electrodes of the vertical array and voltage is measured across the adjacent vertical electrodes. Only non-current carrying electrodes are involved in the measurement. Therefore, a total of 104 (4 x 26) measurements are available for each iteration. The true conductivities of the top, middle and bottom layer are set to 0.15 mS/cm, 0.125 mS/cm, and 0.1 mS/cm, respectively. The contact impedance of 0.35  $\Omega \times \text{cm}^2$  is used. The time between the consecutive measurements is set to one min. Different meshes are used for forward and inverse solver in order to avoid *inverse crime*. Forward solver was used to compute the boundary voltages using 4401 nodes and 19672 tetrahedral elements. On the other hand, 3885 nodes and 17705 tetrahedral elements were used in inverse solver. In generating the voltage data 1% Gaussian noise is added to emulate the real situation. Extended Kalman filter and unscented Kalman filter are used as inverse algorithms in estimation and the performance is compared. The results for phase interface estimation are shown in Figure 2, it can be seen that, UKF has better estimation compared to EKF. The upper interface is estimated better by UKF. On the other hand the lower interface estimation has little problem at the end. It is due to lower value of the estimated conductivity of the bottom layer (Figure 4). The reconstruction results for the interface velocities are given in Figure 3. UKF has better estimation of interface velocities as compared to that of EKF. In regard to the conductivities (Figure 4), the estimation performance of UKF for upper and middle

conductivities is better than EKF. However, lower conductivity estimation is relatively poor in both UKF and EKF. By using UKF as an inverse solver, there are several performance gains over conventional extended Kalman filter (EKF). In the case of UKF, the mean and covariance of the state estimate is calculated up to second order where as in EKF it is accurate up to first order. Therefore, UKF always gives better results as compared to EKF. Secondly, no analytical Jacobian is needed to be calculated, as the key point in UKF is the nonlinear unscented transform which uses the nonlinear measurement equation as such.

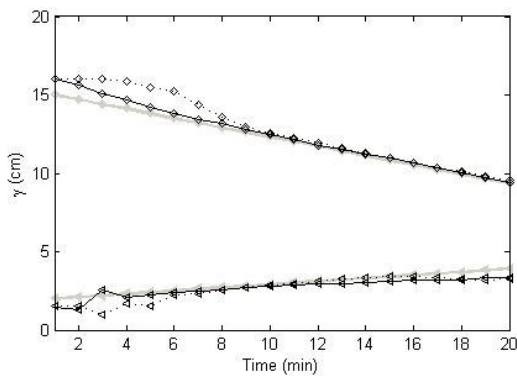


Figure 2. Phase interface location for the test case. (Gray line represents the true interface location, black line represents the estimated phase interface, solid represents UKF, and dotted line represents EKF. Diamond ( $\diamond$ ), triangle ( $\Delta$ ), represents the location of upper and lower interface.)

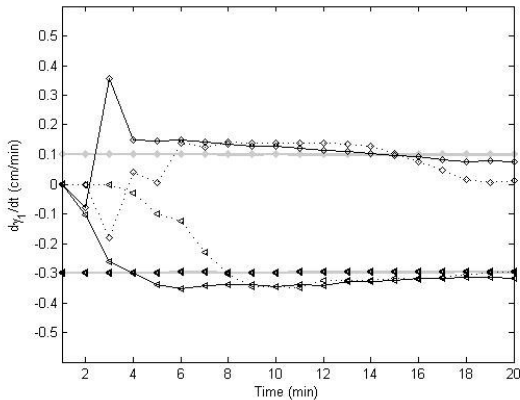


Figure 3. Settling velocities for the test case. (Gray line represents the true velocity, black line represents the estimated velocities, solid represents UKF, and dotted line represents EKF. Diamond ( $\diamond$ ), triangle ( $\Delta$ ), represents the velocities of upper and lower interface.)

## 6. Conclusions

In this paper, the UKF was used to estimate the interface location. To locate the interfacial phase boundaries we use first-order kinematic model as an evolution model. Also, the evolution of interface boundary using kinematic model can be used as *a priori* information and can be incorporated into state equation to obtain better estimation of interface locations. Furthermore, the rate of change of phase interfaces, i.e., settling velocities can be incorporated as a

state parameter and therefore we can obtain the settling velocities as a part of the solution directly without the need of post differentiation of phase interface locations. Extensive numerical experiments have been carried out for the verification of the proposed approach. Results show that the proposed unscented Kalman filter approach has better estimation of the phase interface locations, interface velocities and the conductivity values as compared to extended Kalman filter.

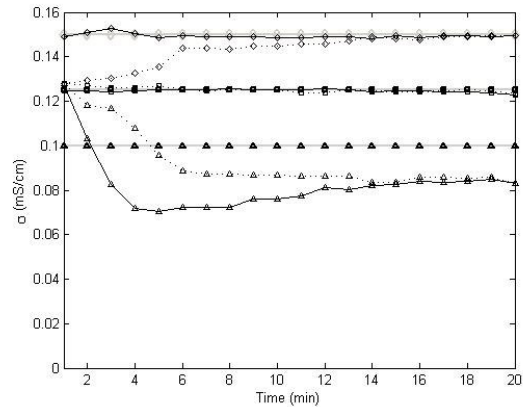


Figure 4. Phase conductivities for the simulated test case. (Gray line represents the true conductivities and black line represents the estimated conductivities, solid represents UKF, dotted line represents EKF. Diamond ( $\diamond$ ), square ( $\square$ ), triangle ( $\Delta$ ), represents the conductivities of upper, middle and lower phase layer.)

## References

- [1] S.J. Julier and J.K. Uhlmann, "Unscented filtering and nonlinear estimation" *Proc. IEEE* vol. 92, pp.401-422, 2004.
- [2] O.P. Tossavainen, M. Vauhkonen and V. Kolehmainen. "A three-dimensional shape estimation approach for tracking of phase interfaces in sedimentation processes using electrical impedance tomography". *Meas.sci.Technol.*, vol. 18, pp.1413-1424, 2007.
- [3] O.P. Tossavainen, M. Vauhkonen, V. Kolehmainen and K.Y. Kim. "Tracking of moving interfaces in sedimentation processes using electrical impedance tomography" *Chemical Engineering Science.*, vol. 61, pp.7717-7729, 2006.
- [4] H. Yoshida, T. Nurtono and K. Fukui. "A new method for the control of dilute suspension sedimentation by horizontal movement" *Powder Technol.*, vol.150, pp. 9-19, 2005.
- [5] D.A. White and N. Verdone. "Numerical Modeling of sedimentation processes" *Chem.Eng.Sci.*, vol. 55, pp. 2213-2222, 2002.
- [6] G.T. Bolton, C.H. Qiu, and M. Wang. "A novel electrical tomography sensor for monitoring the phase distribution in industrial reactors" *In 7 th UK conference on mixing*, Bradford, UK, 2002.
- [7] F.Ricard, C. Brechtelsauber, X.Y. Xu, and C.J. Lawrence. "Monitoring of multiphase pharmaceutical processes using electrical resistance tomography" *Ceresdes*, vol. 83, pp.794-805, 2005.
- [8] X. Rong Li. "Canonical transform for tracking with kinematic models" *IEEE trans. Aerospace and Electronic Systems*, vol. 33, pp.1212-1224, 1997.
- [9] Y. Bar-Shalom and X.R. Li. *Estimation and Tracking: Principles, Techniques and Softwares*, Artech House, 1993.